Atomic Dissection of the Hydrogen Bond Network for Transition-State Analogue Binding to Purine Nucleoside Phosphorylase†

Greg A. Kicska,‡ Peter C. Tyler,§ Gary B. Evans,§ Richard H. Furneaux,§ Wuxian Shi,‡ Alexander Fedorov,‡ Andrzej Lewandowicz,‡ Sean M. Cahill,‡ Steven C. Almo,‡ and Vern L. Schramm*,‡

Department of Biochemistry, Albert Einstein College of Medicine, 1300 Morris Park Avenue, Bronx, New York 10461, and Carbohydrate Chemistry Team, Industrial Research Ltd., Lower Hutt, New Zealand

Received August 14, 2002; Revised Manuscript Received October 8, 2002

ABSTRACT: Immucillin-H (ImmH) and immucillin-G (ImmG) were previously reported as transition-state analogues for bovine purine nucleoside phosphorylase (PNP) and are the most powerful inhibitors reported for the enzyme (K_i* = 23 and 30 pM). Sixteen new immucillins are used to probe the atomic interactions that cause tight binding for bovine PNP. Eight analogues of ImmH are identified with equilibrium dissociation constants of 1 nM or below. A novel crystal structure of bovine PNP−ImmG−PO_4 is described. Crystal structures of ImmH and ImmG bound to bovine PNP indicate that nearly every H-bond donor/acceptor site on the inhibitor is fully engaged in favorable H-bond partners. Chemical modification of the immucillins is used to quantitate the energetics for each contact at the catalytic site. Conversion of the 6-carbonyl oxygen to a 6-amino group (ImmH to ImmA) increases the dissociation constant from 23 pM to 2.6 million pM. Conversion of the 4′-imino group to a 4′-oxygen (ImmH to 9-deazainosine) increases the dissociation constant from 23 pM to 2.0 million pM. Substituents that induce small pK_a changes at N-7 demonstrate modest loss of affinity. Thus, 8-F or 8-CH_3-substitutions decrease affinity less than 10-fold. But a change in the deazapurine ring to convert N-7 from a H-bond donor to a H-bond acceptor (ImmH to 4-aza-3-deaza-ImmH) decreases affinity by $>10^7$. Introduction of a methylene bridge between 9-deazahypoxanthine and the iminoribitol (9-(1′-CH_2)-ImmH) increased the distance between leaving and oxacarbenium groups and increased K_i to 91 000 pM. Catalytic site energetics for 20 substitutions in the transition-state analogue are analyzed in this approach. Disruption of the H-bond pattern that defines the transition-state ensemble leads to a large decrease in binding affinity. Changes in a single H-bond contact site cause up to 10.1 kcal/mol loss of binding energy, requiring a cooperative H-bond pattern in binding the transition-state analogues. Groups involved in leaving group activation and ribooxacarbenium ion stabilization are central to the H-bond network that provides transition-state stabilization and tight binding of the immucillins.

Kinetic isotope effect analysis of bovine PNP predicted that the transition-state structure for this concerted reaction has ribooxacarbenium character in the ribosyl group and an elevated pK_a for the purine leaving-group, with little nucleophilic participation from the phosphate anion (*1*−*3*). On the basis of this information, ImmH[1] and ImmG were synthesized to approximate the features of the transition state (*4*−*6*). Inhibition of bovine PNP[1] was found to be slow-onset, slow-release with thermodynamic equilibrium dissociation constants of 23 and 30 pM, respectively (Figure 1; *7*, *8*). The X-ray structure of bovine PNP−ImmH−PO_4 differed significantly from Michaelis-analogue complexes by numerous favorable hydrogen-bond contacts between the enzyme and inhibitor (*9*−*11*). The substrate inosine and transition-state analogue ImmH are isosteric, differing by only two atoms, N-9 → C-9 and O-4′ → N-4′. These changes increase the affinity from a 17 μM K_m for inosine to a 23 pM K_i* for ImmH, a difference of −8.2 kcal/mol (Figure 1). Increased binding energy with this inhibitor has been attributed to seven hydrogen bonds that are shorter by more than 0.2 Å each in comparing the X-ray crystal structures of PNP−ImmH−PO_4 to PNP−inosine−SO_4. Here we ex-

† This work was supported by Research Grant GM41916 and Training Grant GM07288 from the NIH and the Foundation for Research Science and Technology, New Zealand.

* Corresponding author. Telephone: (718) 430-2813. Fax: (718) 430-8565. E-mail: vern@aecom.yu.edu.

‡ Albert Einstein College of Medicine.

§ Industrial Research Ltd.

[1] Abbreviations: The trivial name immucillin indicates 9-deazapurine in a C-9 to C-1′ carbon−carbon bond to 1,4-dideoxy-1,4-imino-D-ribitol (see atomic numbering in Figure 1). Specific immucillin analogues are named to indicate modifications in the 9-deazapurine and the imino-ribitol groups. Examples include the following: ImmH (immucillin-H, [(1*S*)-1-(9-deazahypoxanthin-9-yl)-1,4-dideoxy-1,4-imino-D-ribitol]), where H indicates 9-deazahypoxanthine; ImmG (immucillin-G, [(1*S*)-1-(9-deazaguanin-9-yl)-1,4-dideoxy-1,4-imino-D-ribitol]), where G indicates 9-deazaguanine; ImmA (immucillin-A, [(1*S*)-1-(9-deazaadenin-9-yl)-1,4-dideoxy-1,4-imino-D-ribitol]), where A indicates 9-deazaadenine; 2′-d-ImmH (2′-deoxy-immucillin-H, [(1*S*)-1-(9-deazahypoxanthin-9-yl)-1,2,4-trideoxy-1,4-imino-D-ribitol]); Δ2-ImmH (C2-deleted-immucillin-H, [(1*S*)-1-(3-amino-2-carboxamidopyrrol-4-yl)-1,4-dideoxy-1,4-imino-D-ribitol]). Other abbreviations for immucillins, together with the structures, are indicated in Figure 3. PNP, purine nucleoside phosphorylase; K_i*, dissociation constant for a slow-onset tight binding inhibitor that includes slow onset and release components; K_i, dissociation constant for rapidly reversible binding (initial phase inhibition) of an inhibitor to PNP.

10.1021/bi026636f CCC: $22.00
Published on Web 11/13/2002

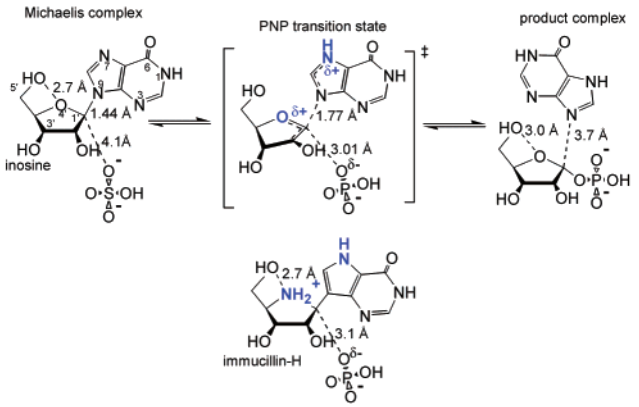

FIGURE 1: The reaction catalyzed by PNP and the bond lengths in the reaction coordinate from crystal structures and transition-state analysis. The structures of PNP−inosine−SO_4, transition state, product complex, and PNP−ImmH−PO_4 have been reported (*2*, *3*, *10*, *11*). The major changes on conversion of substrate to transition state are indicated in blue and are highlighted in immucillin-H. ImmH is shown as the N4′-protonated cation, based on the H-bond patterns of the ImmH and ImmG complexes in Figure 2b,c. The 3.7 Å separation between N9 of hypoxanthine and C1 of ribose 1-PO_4 in the product complex is a consequence of the electrophile migration mechanism in which C1′ translates from the purine ring toward the phosphate (*11*).

amine atomic substitutions in ImmH and correlate the changes in affinity with individual interactions characterized in the crystal structure (*11*). The crystal structure of PNP with ImmG is also reported here to define the interactions with the exocyclic amine and analogues of ImmG.

The results establish that the high-affinity binding of ImmH and ImmG is not the result of single interactions, but results from a constellation of cooperative hydrogen bond interactions, all of which are required to form the tightly bound complex. However, the binding energy of the transition-state analogue can be eliminated by changes to a single H-bond, especially when these contribute to the electrostatic nature of the transition state. Analysis of transition-state analogue binding energies by atomic interrogation is analogous to catalytic site analysis by site-directed mutagenesis but removes the uncertainty of modifying the protein structure with the mutations.

MATERIALS AND METHODS

Reagents. Immucillin-H [(1*S*)-1-(9-deazahypoxanthin-9-yl)-1,4-dideoxy-1,4-imino-D-ribitol] and related immucillins were synthesized from D-gulonolactone and chemically protected 9-deazapurine bases, or were synthesized by sequential additions to protected iminoribitols as described previously (*6*, *12*). [7-^{15}N]Immucillin-H was prepared by the introduction of ethyl[^{15}N]aminoacetate at the step incorporating N7. Structure and mass of analogues were established by NMR and mass spectrometry, and purity was confirmed by HPLC. Inosine, xanthine oxidase and purified calf spleen PNP were purchased from Sigma (St. Louis, MO). For NMR and crystallographic studies, PNP was further purified to near homogeneity by affinity chromatography (*13*).

Catalytic Activity Assays. Purified enzyme preparations provided by the manufacturer (see above) were used directly in inhibition and kinetic studies. Enzyme purity for kinetic and inhibition studies was approximately 80% by denaturing polyacrylamide gel electrophoresis. Catalytic activity was determined at 30 °C in 50 mM KPO_4, pH 7.4, with variable inosine concentration (40 μM to 5 mM). In a coupled assay, hypoxanthine was converted to uric acid by the presence of 160 milliunits/ml of xanthine oxidase. The reaction is followed by measuring uric acid formation at 293 nm with $E_{293} = 12.9$ mM cm^{-1} (*14*). Individual experiments were conducted to establish that the reaction rates were not influenced by the interactions of the inhibitors with xanthine oxidase.

Inhibition Studies. Initial reaction rates were measured by addition of enzyme to complete assay mixtures. Substrate concentration was adjusted so that suitable reaction rates could be obtained with inhibitor concentration at least 10-fold greater than enzyme concentration. Tight-binding inhibitors exhibit two phases of inhibition. The initial rate inhibition is the reversible competitive binding with respect to substrate, and is described by the dissociation constant K_i, from fits to the equation; $v_o = (k_{cat}A)/(K_m(1 + I/K_i) + A)$, where v_o is the inital reaction rate, K_m is the Michaelis constant, A is the substrate concentration, and I is the inhibitor concentration. Slow-onset inhibition may occur following the initial rate period and results in a second steady-state phase at a lower reaction rate. These second slopes are used to determine K_i* by fitting to the equation for competitive inhibition; $v_s = (k_{cat}A)/(K_m(1 + I/K_i^*) + A)$, where v_s is the steady-state rate following completion of slow-onset inhibition and K_i* is the equilibrium dissociation constant for the tightly bound enzyme−inhibitor complex (*15*, *16*). Examples of these slow-onset kinetic curves and the kinetic analysis for bovine PNP are illustrated in Miles et al. (*8*). The K_m value under the conditions used for inhibitor assays was measured to be 17 μM.

Energetics of Inhibitor Binding. Differences in Gibbs free energy for binding of inhibitors or substrate were compared for ligand pairs using the expression $\Delta G^\circ = RT \ln[K_1/K_2]$, where K_1 and K_2 are dissociation constants for the test and reference compounds, respectively. For purposes of this expression, K_m was assumed to be a dissociation constant, which is only an approximation of the true value, since bovine PNP is known to demonstrate forward commitment to catalysis with inosine and to have release of the purine-base product as a slow step in the catalytic cycle (*2*, *17*). When K_1 and K_2 are for competitive inhibitors, the comparison is thermodynamically correct.

Crystallography of PNP−ImmG−PO_4. The methods and conditions for growth of crystals, collection of data, and determination of the structure are the same as described earlier for the structure of PNP−ImmH−PO_4, except that ImmG was used in the crystallization drops in place of ImmH (*11*). The complex with ImmG and PO_4 crystallized in the $P2_13$ space group with unit cell dimensions $a = 90.32$ Å and diffracted to 2.0 Å for the complex with ImmG. Data collection was 86.8% of the complete set at 2.0 Å with an R_{sym} of 7.7%. In the 2.00−2.09 Å shell, completeness of the data was 76.8%. The structure was solved by molecular replacement as described previously for the complex with ImmH (*11*). The final model included residues 2−279, ImmG, phosphate, a Mg^{2+} ion (from the crystallization medium, and remote from the catalytic site), and 145 water molecules. Final R_{crys} and R_{free} were 0.164 and 0.246, respectively. The model displayed good stereochemistry with 91.5%, 7.7%, 0.4%, and 0.4% of amino acid geometries in

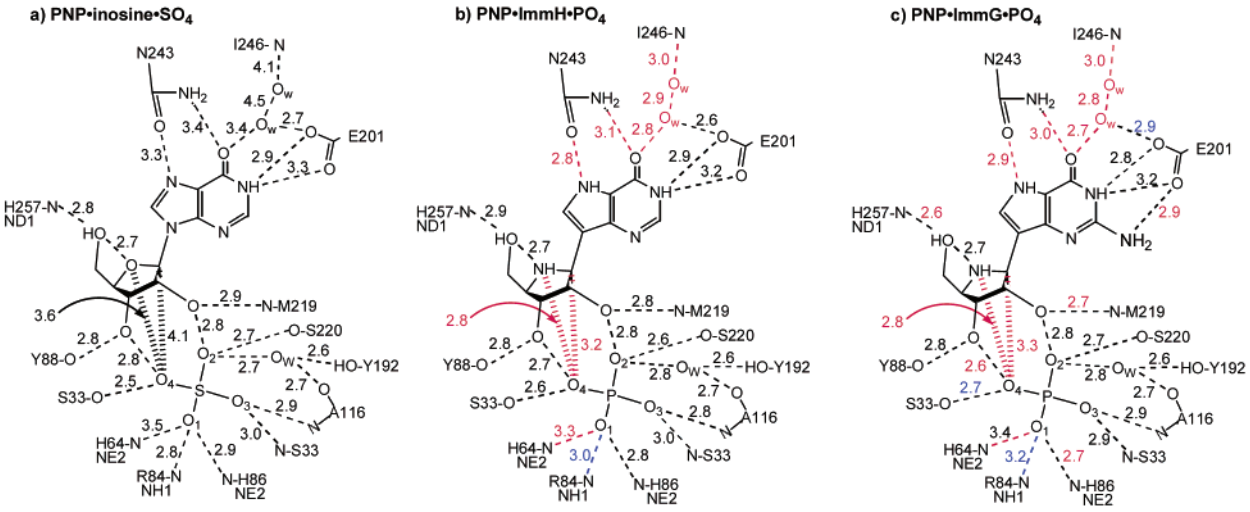

FIGURE 2: Noncovalent contacts in the complexes bovine PNP−inosine−SO_4, PNP−ImmH−PO_4 and PNP−ImmG-PO_4. The distances (in Å) in panels a and b are from Protein Data Base files 1A9S and 1B8O, while that reported in panel c is available from PDB file 1B8N. Interactions shown in panels b and c that are 0.2 Å or more closer than that in panel a are shown in red, and those that are 0.2 Å or more distant in panels b and c than in panel a are shown in blue. All contacts of 3.0 Å or closer are shown, together with selected contacts >3.0 Å for important interactions.

the most favored, additional allowed, generously allowed, and disallowed regions, respectively. The single residue in the category of disallowed geometry is Thr221. It demonstrates good electron density in omit maps and is in the same geometry in the structure of PNP−ImmH−PO_4 solved previously to 1.5 Å. Thr221 is adjacent to Ser220, whose side chain hydroxyl shares 2.6 and 2.7 Å hydrogen bonds to phosphate in complexes with ImmH and ImmG, respectively. The coordinates for bovine PNP in complex with phosphate and ImmG have been deposited with the Protein Data Base code 1B8N. The complex with phosphate and ImmH has PDB code 1B8O.

1D ^{1}H NMR of ImmH and Complexes. [7-^{15}N]Immucillin-H was dissolved in 10% D_2O containing 50 mM KPO_4, pH 7.4, and the NMR spectra were collected at 308 °K for 2048 scans on a 600 MHz Bruker Avance spectrometer using a 1−1 experiment with an excitation maximum at 15 ppm and an excitation null at the water resonance. Purified PNP in the same buffer was concentrated to 30 mg/mL and diluted to a final concentration of 670 μM with 10% D_2O. After the spectra of the PNP−PO_4 complex was collected, the solution was made to 670 μM with [7-^{15}N]ImmH, and additional spectra taken as a function of temperature (2048 scans). NMR experiments were conducted to locate downfield protons coupled to the ^{15}N. The ^{15}N-edited proton spectrum was acquired using a one-dimensional version of the HMQC experiment where all hard 90° and 180° pulses were replaced by their 1−1 counterparts. A total of 32 000 transients were collected. All chemical shifts were referenced to internal 3-trimethylsilyl-propionate. Additional details are provided in the legend to Figure 4.

Gaussian Calculations. Molecular cutoff models of Δ-C2−ImmH and Δ-C2−PZ−ImmH were optimized for geometry and electron distribution in Gaussian 98 using basis sets 3-21G, 6-31G*, and, in one case, DFT:B1Lyp/6-31G*. Mulliken charge distribution at H-bonding sites and energetics of carboxamide group rotation were the primary parameters of interest.

RESULTS AND DISCUSSION

Introduction to the Immucillins. Following the discovery of the PNP transition state, ImmH and ImmG were designed, synthesized, and characterized as transition-state analogues (*7*). They are powerful inhibitors of human and bovine PNPs, binding up to 10^6 fold tighter than substrates and causing complete inhibition of the bovine PNP when only one of the three catalytic sites is filled (*7*). The crystal structure of bovine PNP−ImmH−PO_4 established catalytic site contacts of a saturated structure with all three sites filled, and comparison with earlier structures revealed that catalysis occurs by C-1′ migration of the ribosyl group (*10*, *11*). The work presented here is a direct extension of the earlier studies by presenting the first characterization of 16 new immucillins with bovine PNP and the crystal structure of bovine PNP−ImmG−PO_4. Interactions for some of these immucillins have been reported for human and malarial PNPs (*18*, *19*) but not the bovine enzyme. Here we compare substrate and transition-state analogue interactions by kinetic and structural analysis to establish the energetic contribution of hydrogen bond pairs in binding transition-state analogues.

Substrate and Transition-State Binding Affinity. Inosine and guanosine bind to form Michaelis complexes with PNP + PO_4, with K_m values of 17 and 13 μM, respectively. ImmH and ImmG are the transition-state analogues for each of these substrates (*7*). The substitutions of carbon for N-9 and nitrogen for O-4′ increases equilibrium binding affinity (K_i*) by factors of 7.4×10^5 and 4.3×10^5, respectively. The two atomic changes in the substrate molecules therefore contribute −8.1 and −7.8 kcal/mol to binding energy. The structural basis for the increased binding affinity of ImmH is summarized in Figure 2 and involves improved H-bond distances at seven or more sites in the PNP complexes with ImmH and ImmG relative to Michaelis complexes (*11*). Thus, the full accounting of transition-state analogue binding energy requires improved H-bond energy of only 1.1−1.2 kcal/mol per altered H-bond interaction. In the atomic alterations of ImmH and ImmG described here, the energetic

contributions of these H-bonds to inhibitor binding energy is evaluated.

Substitutions in the 9-Deazahypoxanthine Ring. The catalytic site of bovine PNP accepts both inosine and guanosine as substrates but is inactive with adenosine or xanthosine (*20*). The enzyme holds the 9-deazahypoxanthine ring of ImmH in close proximity to a loop covering the catalytic site, with hydrogen bonds to N7, O6, and N1. In the Michaelis complexes of inosine + SO_4, interactions to both N7 and O6 are weaker than those in the complex with ImmH + PO_4 (Figure 2; *9*, *11*). The interactions of N243 with N7 and O6 are critical for catalysis since the bovine enzyme is catalytically inactive with adenosine as substrate, and Asn243Ala in the human PNP decreases k_{cat} by a factor of 10^3 for inosine (*20*−*22*). Mutation of Asn243 to Asp decreases efficiency for inosine but permits phosphorolysis of adenosine at about 1% the rate of the native enzyme for inosine (*22*). The interactions of Glu201 at N1 do not change in substrate, transition-state analogue, and product complexes; nevertheless, it is essential for catalysis since mutation of Glu201Ala decreases k_{cat} by 10^{-4} for guanosine (*22*). Likewise, the presence of a C2-amino group in guanosine is accepted for catalysis but the hydroxyl group of xanthosine at this position eliminates substrate activity (*20*).

The H-bond at N7−*Asn243*. Energetics for purine base interactions to PNP can be explored by comparing the equilibrium dissociation constant for ImmH with single atomic substitutions. At the transition state for inosine phosphorolysis, the departing purine base has increased negative charge (electron density) from the bonding electrons, increasing the pK_a of N7 from 1.2 in inosine, to an increased (but unknown) value at the transition state. This electronic change permits H-bond formation between the carboxamide oxygen of Asn243 and N7. ImmH has a pK_a of approximately 9.5 for N7 and is 99% protonated at neutral pH.[2] This protonation is critical to form the H-bond to the carbonyl oxygen of the carboxamide side chain of Asn243. The contribution of this interaction can be tested by moving N3 to the 4 position of the ring, to alter the conjugation pattern of the heterocycle and decrease the pK_a of N7, as seen in 4-aza-3-deaza-ImmH (Figure 3)[3]. The dissociation constant increases from 23 pM for ImmH to 422 million pM for the 4-aza-3-deaza analogue, corresponding to a remarkable 10.1 kcal/mol loss in binding energy. As shown below, this energetic change is not due to the single H-bond at N7, but is a cooperative interaction between this and other H-bonds to the immucillins.

The nature of the interaction between N7 of purine substrates and Asn243 has been confused by the observation that N7-methyl nucleosides (7-methylinosine, 7-methylguanosine and 6-thio-7-methylguanosine) are substrates for PNP (*23*). However, N7 methylation induces a positive charge in the purine ring, and these compounds have a chemically destabilized N-ribosidic bond, rendering the enzymatic activation at N7 unnecessary. The N-ribosidic bond is sufficiently weak that PNP can simply hydrolyze 7-methylguanosine in the absence of PO_4, however phosphate increases the rate. Likewise, nicotinamide-β-D-riboside is an atypical substrate for PNP because of the positively charged and activated leaving group (*17*). The substrate activity of 7-methylnucleosides indicates that the Asn243, located on a flexible region of PNP (*10*), has sufficient mobility to relocate away from the 7-methyl group when purine group activation is not needed. This mobility has limits since constraints on the leaving group pocket prevent PNP from accepting *p*-nitrophenyl O-β-D-ribose as substrate (*24*).

NMR Analysis of the Asn243−*N7 Hydrogen Bond*. The distance between the oxygen and nitrogen in the Asn243−N7 hydrogen bond is 2.8 Å, within crystallographic error of strong hydrogen bonds that demonstrate downfield chemical shifts (*25*). In the 2.0 Å structures of the hypoxanthine−guanine phosphoribosyltransferases from human and malarial sources, a 2.8 Å hydrogen bond is present between a carboxylate oxygen of an Asp at the same position of Asn243 in PNP and N7 of ImmH 5′-phosphate at the catalytic site. NMR proton signals at 13.9 and 14.3 ppm (for the two enzymes) were unequivocally assigned to this hydrogen bond by ^{15}N-edited proton NMR spectra using [7-^{15}N]ImmH 5′-phosphate (*26*−*28*). The NMR spectrum of bovine PNP with bound [7-^{15}N]ImmH and phosphate reveals a downfield H-bond at 15.1 ppm unique to the PNP−ImmH−PO_4 complex. However, an HSQC experiment to measure protons coupled to ^{15}N-spins demonstrated that the downfield hydrogen bond does not originate from this interaction (Figure 4).

The 10.1 kcal/mol difference in binding energy between ImmH and 4-aza-3-deaza-ImmH is not the result of a single H-bond to N7. However, this bond is necessary to foster the cooperative interaction of optimal H-bonds at other sites in the ImmH molecule. The assignment of the 15.1 ppm H-bond signal has not yet been made, and the 14 hydrogen bonds of 2.8 Å or less in the complex make this assignment an experimental challenge.

Changing the pK_a at N7. Substituents placed at C8, adjacent to N7 cause small changes in the pK_a value for N7 protonation. Matching of pK_a values for hydrogen bond pairs is proposed to play an important role in transition-state stabilization (*29*, *30*). If the pK_a of 9.5 for N7 of ImmH is optimal, addition of electron-withdrawing or electron-donating groups at C8 will decrease affinity. Conversely, tighter binding might be expected if the pK_a of N7 is shifted to provide a more favorable H-bond pattern at the catalytic site. The pyrazolopyrimidine analogue PZ-ImmH exhibits slow-onset inhibition and binds with a K_i* of 40 pM, not substantially different from the parent ImmH. Substitution of C8 with methyl or fluoro groups to give 8-Me−ImmH and 8-F−ImmH results in inhibitors that retain the slow-onset, tight-binding inhibition pattern but increase the K_i* values to 90 and 140 pM, respectively. Since each of these substitutions at C8 decrease the binding slightly, the pK_a of the N7 of ImmH is likely to be near the optimal value to stabilize formation of the transition-state analogue complex. The pK_a values of the N7 positions of PZ−, 8-Me−, and 8-F−immucillins have not yet been established due to lack

[2] The pK_a values for ImmH were determined by pH titration, following the NMR spectra of [1′-^{13}C], [1′-^{1}H], and [4′-^{15}N]. NMR studies on the enzyme are in progress (Sauve, A. A., Cahill, S. M., Girvin, M. E., and Schramm, V. L. (2002) unpublished results).

[3] A single atomic numbering system is used in discussing the inhibitor molecules. Atomic numbering of the purine and ribosyl rings of inosine and guanosine is imposed on the immucillin ring systems, even when the rings are open or are substituted in ways that alter IUPAC-recommended numbering systems.

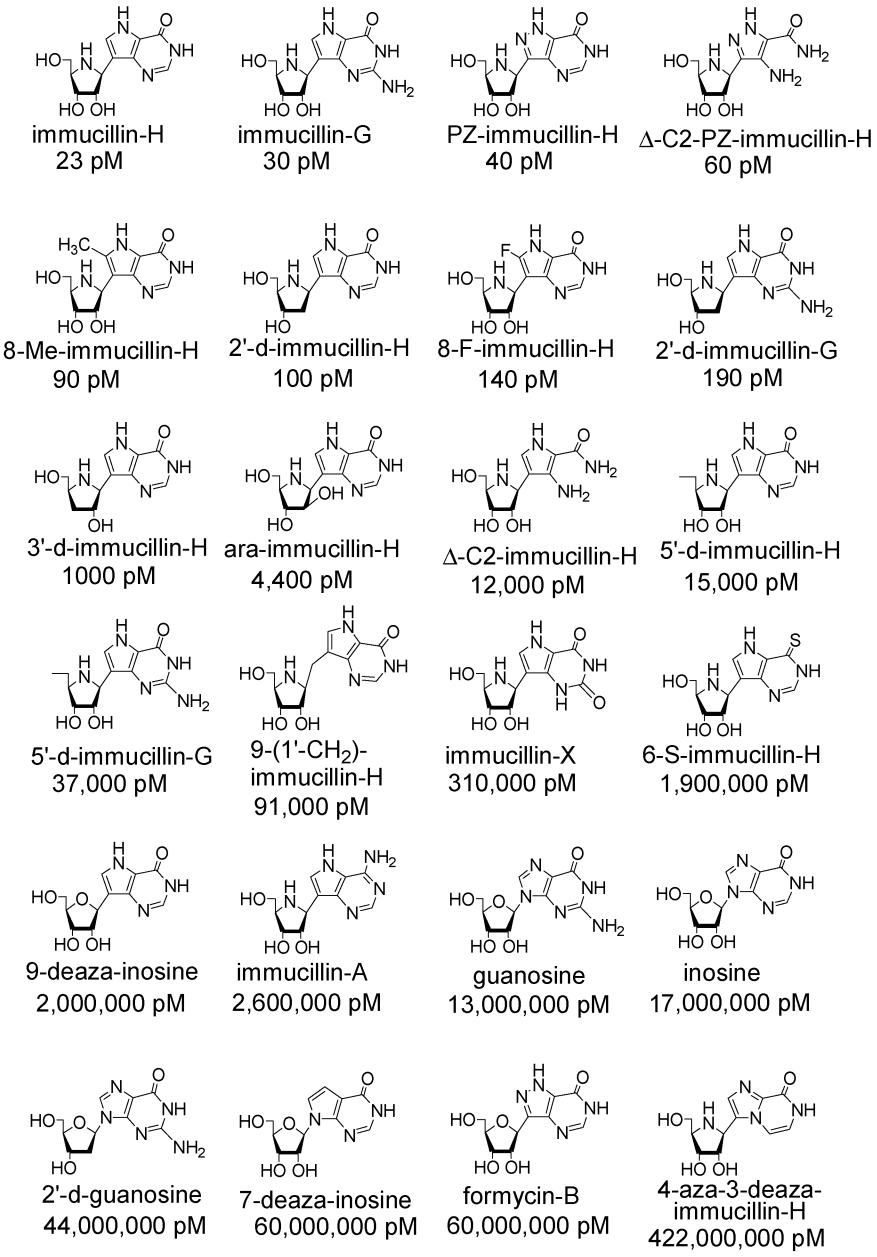

FIGURE 3: Transition-state analogues, substrates, and competitive inhibitors for PNP. The values shown below each compound are equilibrium dissociation constants. Inhibitors with dissociation constants of 1000 pM or below generally display inhibition in two phases defined by the constants K_i and K_i* (see the Methods), while those above this value exhibit a single phase inhibition. Values reported here are the smaller of the values, reflecting the final equilibrium dissociation constants. Constants for ImmH, ImmG, 9-deaza-inosine, guanosine, inosine, 2′-d-guanosine, 7-deazainosine and formycin-B were reported earlier, as referenced in the text. All other immucillin interactions with bovine PNP are novel to this work.

of sufficient material but provide an obvious avenue for extension of this inhibitor design program.

Interaction of Glu201 with O6 and N1. Hydrogen bonds between Glu201 and several immobilized water molecules in contact with ImmH form a well-ordered network between the protein, O6, and N1 of the six-membered ring (Figure 2). Asn243 is also involved at O6 as a 3.1 Å H-bond donor. Many of these contacts tighten substantially on formation of the complex with ImmH, and Glu201 is known to be important for catalysis (*9*; see above). The single atom substitution of a sulfur for O6 explores the nature of the hydrogen bonds to O6, and demonstrates a change from 23 pM for ImmH to 1.9 million pM for 6-S−ImmH, a 5.7 kcal/mol energetic loss as a result of this change. Thiols form weak hydrogen bonds, and the loss of the O6-centered H-bond pattern causes the binding to decrease from the pM range toward the μM affinity of substrates, where the H-bond pattern around O6 is weak (Figure 2).

Conversion of the 6-oxy of ImmH to the 6-amino of ImmA changes the 6-substituent from a H-bond acceptor to a donor and also changes the protonation pattern at N1. Both of these changes disrupt the H-bond pattern centered around Glu201 and change the affinity from 23 pM for ImmH to 2.6 million pM for ImmA, a loss of 5.9 kcal/mol in binding energy. Thus, a major energetic contribution to the binding of immucillin analogues comes from the H-bond network surrounding O6 and N1. This network is proposed to provide a proton-transfer bridge that donates the protons for the transition-state

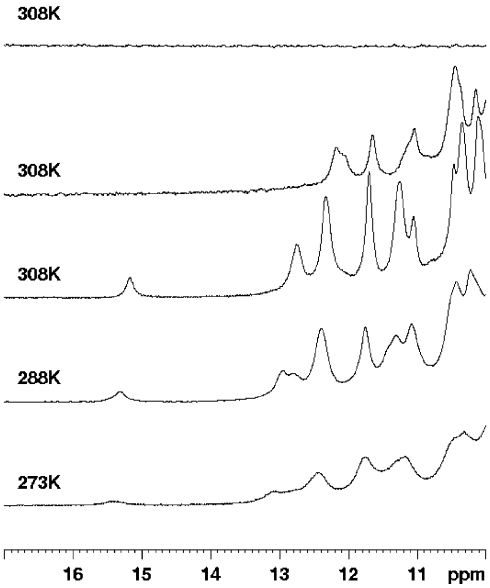

FIGURE 4: 1D ^{1}H NMR spectra of PNP in complex with [7-^{15}N]-ImmH and phosphate. The lower three spectra, labeled 273K, 288K, and 308K, are the 10−17 ppm downfield spectra of 670 μM bovine PNP and equimolar [7-^{15}N]ImmH containing 50 mM KPO_4 buffer, pH 7.4, at increasing temperatures. The second spectrum from the top labeled 308K is the same PNP sample before [7-^{15}N]ImmH is added. These spectra were 1−1 experiments, with excitation maximum at 15 ppm. A total of 2048 transitents were collected (*41*). The top spectrum is an ^{15}N-edited spectrum using a one-dimensional version of the HMQC experiment as described in the methods and elsewhere (*42*). Protons coupled to ^{15}N would provide a single peak at the same chemical shift as in the lower spectra. Control experiments with [7-^{15}N]ImmH in the buffer alone show the proton coupled to the [7-^{15}N] at 11.7 ppm (not shown). Chemical shifts for ImmH in H_2O/D_2O give proton spectra with 8.06 and 7.66 ppm as the most downfield protons from H2 and H8, respectively. Spectra were collected using 10% D_2O as the lock signal. Similar experiments with hypoxanthine−guanine phosphoribosyltransferases and [7-^{15}N]ImmH 5′-PO_4 have established positive control results for this experiment (*26*, *28*)

hydrogen bonds to both N7 and O6 (*11*). Disruption of this pattern prevents catalysis and tight-binding of transition-state inhibitor analogues.

Rigid versus Open Ring Systems. Deletion of C2 from the 9-deazapurine ring of ImmH gives Δ-C2−ImmH and changes N1 to a carboxamide group. The ability of O6 to form hydrogen bonds will now be affected by the rotational freedom of the carboxamide group and internal H-bonds that may form between the carboxamide oxygen and the N3 amino group.[3] These changes reduce the affinity of ImmH from 23 pM to 12 000 pM for Δ-C2−ImmH, a change of 3.8 kcal/mol. The same strategy applied to PZ−ImmH gives Δ-C2−PZ−ImmH. The dissociation constants of 40 pM and 60 pM are not significantly changed in the case of the pyrazolo derivatives. The reasons for the differences between the ImmH and PZ−ImmH analogues with respect to deletion of C2 are not established but may relate to differences in the H-bond potential for the carboxamide oxygen as a result of the pyrazolo group. Gaussian 98 calculations were conducted to determine the optimal geometry and the electron distributions of model compounds of Δ-C2−ImmH and Δ-C2−PZ−ImmH. In the computational models, the iminoribitol group is replaced by a methyl group, and computations were conducted at the basis sets indicated in the methods. The Mulliken charge distribution on the carboxamide oxygens is −0.651 and −0.631 for Δ-C2−ImmH and Δ-C2−PZ−ImmH, respectively; thus, the Δ-C2−PZ−ImmH is a weaker hydrogen bond acceptor at this site. The charge at the N7 proton changes only slightly, from 0.421 to 0.429 for the same pair. These differences may bias the disposition of the carboxamide group in the catalytic site and thereby account for the differences in binding energy. Additional crystallographic analysis will be required to establish the structural basis for this difference.

Substitutions at C2. Inosine and guanosine are good substrates for bovine PNP, and ImmH, and ImmG are equally powerful as transition-state analogues at 23 and 30 pM, respectively. These values suggest the possibility that catalytic site contacts to the C2 substituent are weak and that other C2 substituents would serve equally as transition-state analogues. ImmX replaces the C2 exocyclic amine with a carbonyl oxygen, and decreases the affinity from 30 pM in ImmG to 310 000 pM in ImmX for a decrease in binding energy of 5.5 kcal/mol. The X-ray crystal structure of bovine PNP with ImmG and PO_4 bound at the catalytic site establishes that contacts to the exocyclic amine are an extension of the H-bond network to Glu201 with an additional 2.9 Å H-bond from the C2 amine to a carboxylate oxygen of Glu201 (Figure 2c, 5). Substitution of an exocyclic oxygen at C2 prevents this interaction, disrupting the H-bond network to cause a 5.5 kcal/mol loss of binding energy. The interaction of ImmG at the catalytic site is similar to that reported for other guanine analogues with respect to the Glu201 interaction (*9*), except that the H-bonds to the inhibitor are strengthened in the same manner as those to ImmH in comparison to analogues of the Michaelis complex. Within the limits of crystallographic resolution, complexes of ImmH and ImmG establish the same contacts at the catalytic site with two exceptions. A new 2.9 Å H-bond forms between Glu201 and the C2-amino group, and the H-bond between the Glu201 carboxylate oxygen and the water in contact with O6 increases from 2.6 Å with ImmH to 2.9 Å with ImmG (compare panels a and c of Figure 2). Since the affinity of ImmH and ImmG are equivalent, these two changes in H-bond strengths provide equivalent and opposite contributions to transition-state analogue binding. Since inosine and guanosine are equivalent substrates, this H-bond pattern is also energetically equivalent in contributions to the rate-limiting step for PNP catalysis, namely, the release of hypoxanthine and guanine. If the energetic contributions to transition-state formation are also the same, pre-steady-state catalysis purine formation on the enzyme would occur at equivalent rates.

Energetics of N9 Substitution. The chemical stability inherent in the immucillins stems from the 9-deaza substitution, which also alters the pK_a of N7, as indicated above. The effect of this substitution alone can be considered by comparing interactions of inosine, 9-deazainosine, 4-aza-3-deaza-ImmH, and ImmH with PNP. If the increased binding affinity of ImmH arises primarily from the increased pK_a at N7, 9-deazainosine would be expected to bind tightly. Inosine has a K_m of 17 μM, while 9-deazainosine inhibits with a dissociation constant of 2 μM (*17*). The K_m for inosine is greater than the dissociation constant, and forward commitment factors established that the first turnover for arsenolysis of inosine is 10-fold greater than k_{cat}, indicating that K_m is 10 times greater than K_d for the arsenolysis reaction (*2*, *3*).

Thus, the binding affinity of inosine and 9-deazainosine are equivalent. ImmH and 9-deazainosine differ only in the replacement of the 4′-imino group. The ImmH analogue with N3 and C4 reversed tests interactions at N7, since PNP does not interact at N3 (Figure 2). The weak binding of 3-deaza-4-aza-ImmH confirms that 9-deaza alone or the 4′-imino group alone does not elicit tight binding. Both are needed to induce the transition-state binding geometry.

Ribosyl Ring Substitutions. Transition-state formation in PNP is characterized by a partially developed ribooxacarbenium ion, a Pauling bond order of 0.36 remaining to the leaving group, and a very low bond order to the attacking phosphate nucleophile (*3*). Transition states for nucleoside phosphorolysis are reached by the combination of leaving group interactions, interactions at the ribosyl group to form the oxacarbenium ion and by the electrostatic contribution from the nearby phosphate anion. Experimental values from kinetic isotope effect studies demonstrated that there is no significant nucleophilic participation of the phosphate at the transition state (*3*). Acid-catalyzed chemical solvolysis of purine nucleosides operates through leaving group activation in which the purine is protonated to the dication, to withdraw bonding electrons from the ribosyl group (*31*). The transition states for chemical solvolysis of purine ribonucleosides are highly dissociative with bond orders to the leaving group lower than that seen for PNP (*32*). The relatively simple H-bond pattern to the purine base suggested that ribooxacarbenium ion formation may be a dominant force in reaching the transition state. However, good leaving groups in O-ribosyl linkage are poor substrates for bovine PNP (*24*). But highly activated purine or pyridine cation leaving groups do serve as substrates (*20*). The crystal structure of ImmH−or ImmG−PO_4 bound to PNP provided the surprising result that the iminoribitol group is stabilized by only three H-bond contacts to the protein, and none of these are within 3.0 Å of the site of oxacarbenium ion formation but form at the 2′-, 3′- and 5′-hydroxyls (Figure 2). The other four interactions to the iminoribitol are neighboring group interactions from the phosphate and from the 5′-hydroxyl interaction to the 4′-imino group and serve to position the 5′-hydroxyl and a phosphate oxygen to sandwich the N4′ position, the site of electron departure to form the ribooxacarbenium ion in ribonucleosides (*11*). Systematic elimination of the each of the hydroxyl groups that hydrogen bond to the enzyme provides estimates of their energetic contribution to the complex.

Binding of 2′-Alterations in the Immucillins. The 2′-hydroxyl groups of ImmH and ImmG in complex with PNP accept a 2.8 Å hydrogen bond from the peptide backbone amide of Met219 and donate a 2.8 Å hydrogen bond to O2 of bound phosphate. Elimination of the 2′-hydroxyl in both 2′-d-ImmH and 2′-d-ImmG decreases the affinity to 100 and 190 pM, respectively, a decrease of only 1 kcal/mol in both cases. The ability to bind 2′-deoxy analogues is expected from the substrate specificity, where 2′-d-inosine and 2′-d-guanosine are good substrates, and from the biological perspective, since the major function of human PNP is to remove 2′-d-guanosine (*33*). A more damaging change to immucillin binding is incorporation of the opposite hydroxyl stereochemistry at C2′ in ara-ImmH. Here, the dissociation constant changes to 4400 pM, giving an energetic penalty of 3.2 kcal/mol. PNP residues at the upper face of the iminoribitol ring are hydrophobic, with Phe159 from the neighboring subunit and the side-chain of Met119 dominating the interactions (Figure 5B). Incursion of the ara-ImmH 2′-hydroxyl into this region is expected to disrupt the hydrophobic packing of these residues, and force the iminoarabitol into an unfavored conformation, both of which decrease binding affinity.

Binding of 3′-d-ImmH. Mammalian PNP evolved to catalyze the phosphorolysis of purine ribosides and 2′-deoxypurine ribosides, and the 3′-hydroxyl is present in all of its biological substrates. The 3′-hydroxyl accepts a 2.8 Å H-bond from Tyr88 and donates a 2.7 Å H-bond to O4 of phosphate. This phosphate oxygen is the nucleophile for phosphorolysis, thus the H-bond pattern here is related to the reaction coordinate. The K_i* value for 3′-d-ImmH is 1000 pM, a 2.3 kcal/mol penalty in binding relative to ImmH. We would therefore expect a mutation in Tyr88 to Phe to reduce catalysis by a similar extent. However, in human PNP, the mutation Tyr88Phe is silent for k_{cat}/K_m; thus, the change in binding affinity between the transition-state analogues ImmH and 3′-d-ImmH is not reflected in catalysis when the atomic mutation is made in the protein (*9*). The rate-limiting step for mammalian PNPs is release of the purine base product from the enzyme (*17*). Thus, changes in the on-enzyme catalytic rate that reflect transition-state interactions are not manifested in steady-state kinetic studies. This analysis predicts that the pre-steady-state burst of product formation on Tyr88Phe at saturating substrate concentration will be reduced, but the steady-state k_{cat} may be nearly unchanged. Atomic substitution of inhibitors reveals changes in transition-state energy that are inaccessible to steady-state kinetics.

Binding of 5′-d-Immucillins. Isotope effect studies with bovine PNP revealed a large normal kinetic isotope effect with [5′-^{3}H]inosine, and it was interpreted as a geometric distortion of the 5′-hydroxyl group at the transition state relative to free inosine (*2*, *3*). This proposal is confirmed in the crystal structures with bound ImmH and ImmG, where the 5′-hydroxyl oxygen is poised 2.7 Å above the 4′-imino nitrogen. The role of His257 has been proposed to be important in positioning the 5′-hydroxyl to serve in destabilizing the electrons at O4′ in the actual transition state (*3*, *11*). However, the significance of this interaction has been questioned by the site-directed mutagenesis of His257 to Ala, where the k_{cat}/K_m for inosine is decreased only by a factor of 20 (*9*). Inhibition by 5′-d-ImmH gave a K_i value of 15 000 pM, a 650-fold decrease in binding relative to ImmH, representing a 3.9 kcal/mol difference in binding energy. If 5′-d-ImmH introduces an atomic change equivalent to the His257Ala mutation, the efficiency of crossing the transition-state barrier should be reduced by a factor of 650. Since product release is rate-limiting for mammalian PNPs, the effect of the His257Ala mutation on the transition-state efficiency can only be measured in pre-steady-state experiments, which are of increased interest with this knowledge of the effect of the 5′-d-ImmH mutation. The energetics of the 5′-deoxy construct was confirmed with 5′-d-ImmG, which gave a K_i value of 37 000 pM, binding 4.3 kcal/mol less favorably than ImmG and in good agreement with the ImmH pair. It should be noted that neither 5′-d-ImmH nor 5′-d-ImmG shows slow-onset, tight-binding characteristics. Loss of the His257 interaction prevents the time-dependent engagement of H-bonds required to form the transition-state

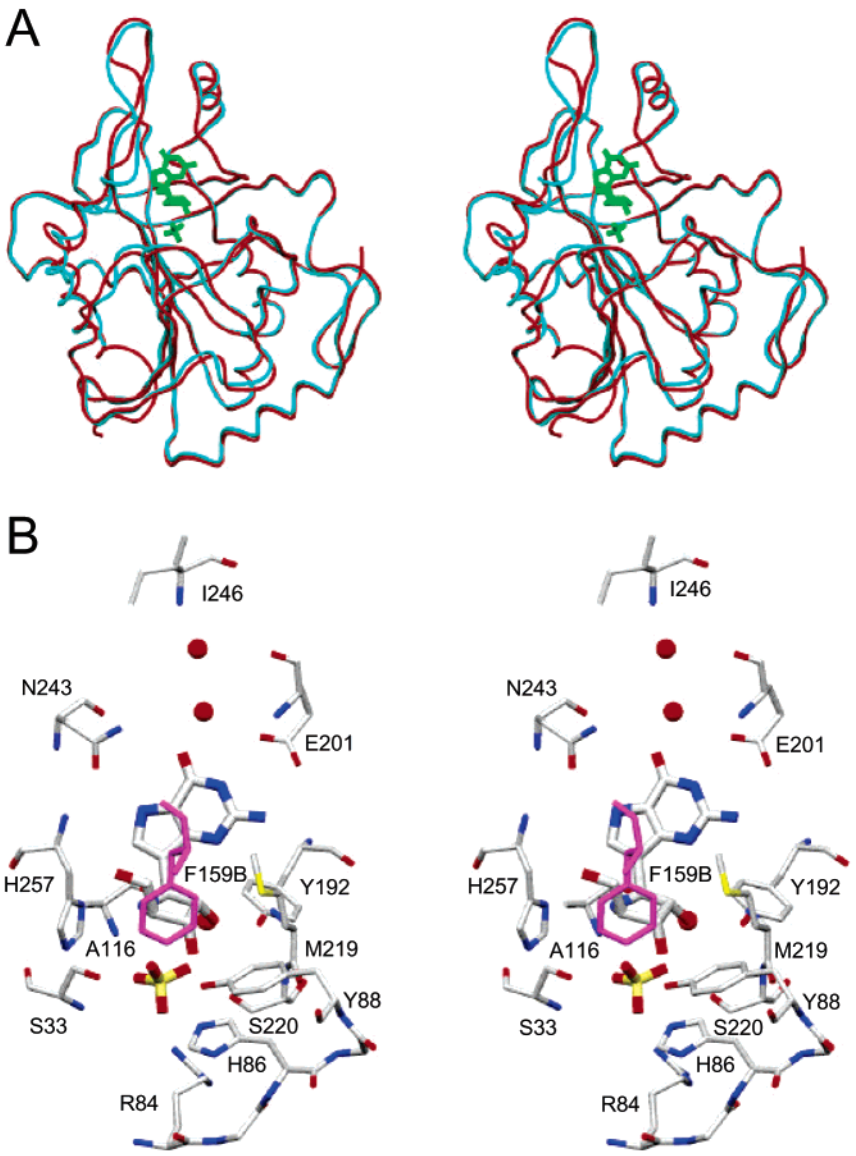

FIGURE 5: Crystallographic structures of PNP in complex with ImmG and phosphate. PNP is a homotrimer, and the stereoview of panel A compares the backbone traces of apoenzyme PNP (in blue, PDB code 1PBN; *10*) to that with bound ImmG and phosphate (in red, PDB code 1B8N) for one of the subunits. ImmG and PO_4 are shown in green. The structures were overlaid using Cα atoms of amino acids 3−279 which give an rms deviation of 1.0 Å. A stereoview of the catalytic site of one subunit of PNP−ImmG-phosphate is shown in panel B. Three structurally significant water molecules are shown as red spheres, and carbon, oxygen, nitrogen, sulfur, and phosphorus atoms are in gray, red, blue, yellow, and green, respectively. The purple residue F159 is from the adjacent subunit and closes over the catalytic site near the top of the iminoribitol ring when ImmG and PO_4 are bound.

ensemble. Crystal structures of these complexes have not yet been obtained, but would be most useful in the interpretation of binding energy.

Contribution of the 4′-Imino Group to Catalysis. ImmH and 9-deazainosine differ by only the 4′-imino group. Both are competitive inhibitors with substrate and permit comparison of equilibrium dissociation constants. For this pair, ImmH binds 87 000 more tightly, to give an energetic contribution of 6.8 kcal/mol as a consequence the 4′-imino group. The same comparison can be made in the pyrazolopyrimidine inhibitors, where PZ-ImmH is compared to formycin-B. The dissociation constants are 40 pM and 60 million pM, respectively. This difference of 1.5×10^6 in binding affinity corresponds to 8.5 kcal/mol in binding energy. Since there are no H-bonds between the enzyme and the imino groups of ImmH or ImmG, we cannot attribute this difference to a specific H-bond to the protein, as has been done with other transition-state analogues (*34*−*36*). However, the imino groups of both inhibitors are positioned to donate 2.7 Å hydrogen bonds to the 5′-oxygen and the O4 of bound phosphate, provided that the immucillin imino groups are protonated when tightly bound to the catalytic sites.

Kinetic and pH profile studies of iminoribitol inhibitors binding to nucleoside hydrolases and to the *Mycobacterium tuberculosis* PNP have established that the initial binding step occurs with the neutral (unprotonated) form of the iminoribitol inhibitors, and preliminary pH profile studies with bovine PNP are also consistent with the binding of neutral ImmH[4] (*37*, *38*). Initial binding of immucillins

[4] The initial phase inhibition (K_i) by ImmH decreased as a function of decreasing pH between 8 and 5. The pK_a for N-4′ protonation is 6.5.[2] (Miles, R. M. and Schramm, V. L. (2002) unpublished results.)

therefore mimics the formation of Michaelis complexes with nucleosides, since both interactions are with neutral substrates. It has been proposed that the slow-onset step leading to tight-binding inhibition involves protonation of the imino group, and computational modeling of nucleoside hydrolase complexes supports this proposal (*39*). Experimental proof of the ionization state of immucillins on enzyme complexes has not yet been reported, but work is progressing toward that goal.[2]

Distance between Leaving Group and Iminoribitol. Transition-state analysis from kinetic isotope effects is a developing technology. It has been suggested that the transition-state structure of PNP may be more highly dissociative than indicated by the kinetic isotope effects reported earlier (*2*, *3*, *40*). The bond between the ribooxacarbenium ion and the leaving group is proposed to be 1.77 Å at the transition state (*3*; Figure 1). A fully dissociated transition state requires both leaving and nucleophilic groups to be greater than 3.0 Å from C1′. However, in ImmH or ImmG, this distance is only 1.5 Å (the length of a C−C bond). Group separation was increased with a methylene bridge between the 9-deazahypoxanthine and iminoribitol groups in 9-(1′-CH_2)-ImmH, which increases the C9 to C1′ distance to 2.5 Å, more closely related to a dissociated transition state (Figures 1 and 3). If the nucleoside at the transition state of PNP is highly dissociated, the binding of 9-(1′-CH_2)-ImmH might be expected to improve relative to ImmH or ImmG. The K_i for 9-(1′-CH_2)-ImmH is 91 000 pM, approximately 4000-fold weaker than that for ImmH. Introduction of the methylene bridge also results in geometric constraints that may affect binding, however, the loss of 5.0 kcal/mol in binding energy indicates that this separation of iminoribitol and deazapurine groups does not create an improved approximation of the transition state.

Summary of Binding Interactions. Complexes of ImmH or ImmG and PO_4 with bovine PNP are characterized by favorable H-bonds to every H-bond donor/acceptor site in the complex except N3. The contacts are closely related to the Michaelis complex of PNP−Inosine−SO_4, except that the hydrogen bond contacts improve with the immucillins. For example, five H-bond contacts to the purine ring of bound inosine are weak interactions (average distance of 3.7 Å), and shorten to favorable interactions (average distance of 2.9 Å) in complexes with the immucillins (Figure 2). Other H-bonds tighten as the immucillins are positioned closer to bound PO_4. Despite more than twenty H-bonds of ≤3.0 Å in the immucillin complexes, a single atomic substitution in the transition-state analogue can disrupt this favorable H-bond pattern and cause large losses of binding energy. Transition-state features of high pK_a at N-7 and the iminoribitol mimic of an oxacarbenium ion are critical (Figure 6).

Cooperative H-bond interactions in the tight binding of immucillins are readily evident from the sum of free energies of binding resulting from individual H-bond disruptions (Figure 6). Thus, the $\Sigma\Delta\Delta G°$ for interactions at the 6-O, N-7 (from C-4 ↔ N-3 switching), O-4′, O-5′, and O-3′ sites is 30 kcal/mol. Catalysis by PNP lowers the transition-state barrier by 10^{14} or less, requiring at most 19 kcal/mol of this interaction energy. The apparent large excess of binding energy from this analysis demonstrates the cooperative nature of individual H-bond interactions with their neighbors, and the actual binding energy is overestimated by such anaylses.

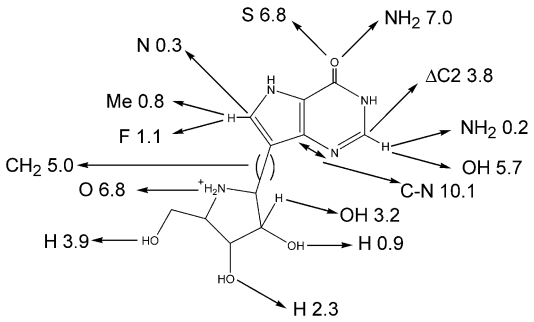

FIGURE 6: Changes of binding energy ($\Delta\Delta G°$ in kcal/mol) for the interaction of immucillin analogues to bovine PNP in the presence of inorganic phosphate. The arrows indicate the atomic changes that lead to the indicated energy changes. Note that H → OH at the 2′ position refers to ara-ImmH, and ΔC2 refers to ΔC-2-ImmH, where deletion of the carbon at C-2 gives N-1 and N-3 as free amino groups. The double-headed arrow between N-3 and C-4 refers to 3-deaza-4-aza-ImmH. The large change in $\Delta\Delta G°$ for this change is a consequence of the pK_a at N-7, not direct interactions at N-3 (see the text).

However, on the basis of the 12 most favorable H-bonds between PNP and bound immucillins (Figures 2b,c), even a modest H-bond energy of 2 kcal/mol provides 24 kcal/mol, a large excess relative to the decrease in transition-state barrier.

CONCLUSIONS

Atomic changes to the immucillin transition-state analogues for PNP alter interactions with catalytic site contacts. Seven immucillins with dissociation constants below 1000 pM have been identified. Tight binding of these transition-state analogues cannot be attributed to any single strong hydrogen bond, although one unassigned downfield H-bond is generated in the complex. Rather, a precise arrangement of H-bond acceptor/donor patterns must be satisfied to cause the enzyme to form an ensemble of favorable H-bond contacts at numerous sites in the immucillin−phosphate complexes relative to Michaelis complexes. The sum of free energy available from these interactions readily exceeds the $\sim 10^{14}$ catalytic rate enhancement imposed by PNP. Disruption of any of any single interaction that prevents transition-state mimicry prevents tight-binding from occurring.

REFERENCES

1. Kline, P. C., and Schramm, V. L. (1992) Purine nucleoside phosphorylase. Inosine hydrolysis, tight binding of the hypoxanthine intermediate, and third-the-sites reactivity, *Biochemistry 31*, 5964−5973.
2. Kline, P. C., and Schramm, V. L. (1993) Purine nucleoside phosphorylase. Catalytic mechanism and transition state analysis of the arsenolysis reaction, *Biochemistry 32*, 13212−13219.
3. Kline, P. C., and Schramm, V. L. (1995) Pre-steady-state transition state analysis of the hydrolytic reaction catalyzed by purine nucleoside phosphorylase, *Biochemistry 34*, 1153−1162.
4. Furneaux, R. H., Limberg, G., Tyler, P. C., and Schramm, V. L. (1997) Synthesis of transition state inhibitors for N-riboside hydrolases and transferases, *Tetrahedron 53*, 2915−2930.
5. Evans, G. B., Furneaux, R. H., Gainsford, G. J., Schramm, V. L., and Tyler, P. C. (2000) Synthesis of Transition State Analogue Inhibitors for Purine Nucleoside Phosphorylase and N-Riboside Hydrolases, *Tetrahedron 56*, 3053−3062.
6. Evans, G. B., Furneaux, R. H., Hutchinson, T. L., Kazar, H. S., Morris, P. E., Jr., Schramm, V. L., and Tyler, P. C. (2001) Addition of Lithiated 9-Deazapurine Derivatives to a Carbohydrate Cyclic Imine: Convergent Synthesis of the Aza-C−Nucleoside Immucillins, *J. Org. Chem. 66*, 5723−5730.

7. Miles, R. W., Tyler, P. C., Furneaux, R. H., Bagdassarian, C. K., and Schramm, V. L. (1998a) One-third-the-sites transition state inhibitors for purine nucleoside phosphorylase, *Biochemistry 37*, 8615−8621.
8. Miles, R. W., Tyler, P. C., Furneaux, R. H., Bagdassarian, C. K., and Schramm, V. L. (1999) Purine nucleoside phosphorylase. Transition state structure, transition state inhibitors and one-third-the-sites reactivity, in *Enzymatic Mechanisms* (Frey, P. A., and Northrop, D. B., Eds.) pp 32−47, IOS Press, Washington, DC.
9. Erion, M. D., Takabayashi, K., Smith, H. B., Kessi, J., Wagner, S., Honger, S., Shames, S. L., and Ealick, S. E. (1997) Purine nucleoside phosphorylase. 1. Structure−function studies, *Biochemistry 36*, 11725−11734.
10. Mao, C., Cook, W. J., Zhou, M., Federov, A. A., Almo, S. C., and Ealick, S. E. (1998) Calf spleen purine nucleoside phosphorylase complexed with substrates and substrate analogues, *Biochemistry 37*, 7135−7146.
11. Fedorov, A., Shi, W., Kicska, G., Fedorov, E., Tyler, P. C., Furneaux, R. H., Hanson, J. C., Gainsford, G. J., Larese, J. Z., Schramm, V. L., and Almo, S. C. (2001) Transition state structure of purine nucleoside phosphorylase and principles of atomic motion in enzymatic catalysis, *Biochemistry 40*, 853−860.
12. Horenstein, B. A., Zabinski, R. F., and Schramm, V. L. (1993) A new class of C-nucleoside analogues. 1-(S)-1,4-dideoxy-1,4-imino-D-ribitols, transition state analogue inhibitors of nucleoside hydrolase, *Tetrahedron Lett. 34*, 7213−7216.
13. Osborne, W. R. (1980) Human red blood cell purine nucleoside physporylase. Purification by biospecific affinity chromatography and physical properties, *J. Biol. Chem. 255*, 7089−7092.
14. Kim, B. K., Cha, S., and Parks, R. E., Jr. (1968) Purine nucleoside phosphorylase from human erythrocytes. I. Purification and properties, *J. Biol. Chem. 243*, 1763−1770.
15. Morrison, J. F., and Stone, S. R. (1985) The behavior and significance of slow-binding enzyme inhibitors, *Comments Mol. Cell. Biophys. 2*, 347−368.
16. Morrison, J. F., and Walsh, C. T. (1988) The behavior and significance of slow-binding enzyme inhibitors, *Adv. Enzymol. Relat. Areas Mol. Biol. 61*, 201−301.
17. Bzowska, A. (2002) Calf spleen purine nucleoside phosphorylase: complex kinetic mechanism, hydrolysis of 7-methylguanosine and oligomeric state in solution, *Biochim. Biophys. Acta 874*, 355−363.
18. Kicska, G. A., Tyler, P. C., Evans, G. B., Furneaux, R. H., Kim, K., and Schramm, V. L. (2002) Transition state analogue inhibitors of purine nucleoside phosphorylase from *Plasmodium falciparum*, *J. Biol. Chem. 277*, 3219−3225.
19. Kicska, G. A., Tyler, P. C., Evans, G. B., Furneaux, R. H., Schramm, V. L., and Kim, K. (2002) Purine-less death in *Plasmodium falciparum* induced by immucillin-H, a transition state analogue of purine nucleoside phosphorylase, *J. Biol. Chem. 277*, 3226−3231.
20. Bzowska, A., Kulikowska, E., and Shugar, D. (2000) Purine nucleoside phosphorylase: properties, functions and clinical aspects, *Pharmacol. Therapeut. 88*, 349−425.
21. Erion, M. D., Stoeckler, J. D., Guida, W. C., Walter, R. L., and Ealick, S. E. (1997) Purine nucleoside phosphorylase 2. Catalytic mechanism, *Biochemistry 36*, 11735−11748.
22. Stoeckler, J. D., Poirot, A. F., Smith, R. M., Parks, R. E., Jr., Ealick, S. E., Takabayashi, K., and Erion, M. D. (1997) Purine nucleoside phosphorylase 3. Reversal of purine base specificity by site-directed mutagensis, *Biochemistry 36*, 11749−11756.
23. Bzowska, A., Kulikowska, E., Darzynkiewicz, E., and Shugar, D. (1988) Purine nucleoside phosphorylase: Structure−activity relationships for substrate and inhibitor properties of N-1-, N-7-, and C-8-substituted analogues; differentiation of mammalian and bacterial enzymes with N-1-methylinosine and guanosine, *J. Biol. Chem. 263*, 9212−9217.
24. Mazzella, L. J., Parkin, D. W., Tyler, P. C., Furneaux, R. H., and Schramm, V. L. (1996) Mechanistic diagnoses for N-ribohydrolases and purine nucleoside phosphorylase, *J. Am. Chem. Soc. 118*, 2111−2112.
25. Mildvan, A. S., Massiah, M. A., Harris, T. K., Marks, G. T., Harrison, D. H. T., Viragh, C., Reddy, P. M., and Kovach, I. M. (2002) Short, strong hydrogen bonds on enzymes: NMR and mechanistic studies, *J. Mol. Struct.* (in press).
26. Li, C. M., Tyler, P. C., Furneaux, R. H., Kicska, G., Xu, Y., Grubmeyer, C., Girvin, M. E., and Schramm, V. L. (1999) Transition state inhibitors for human and malarial hypoxanthine-guanine phosphoribosyl transferases, *Nat. Struct. Biol. 6*, 582−587.
27. Shi, W., Li, C., Tyler, P. C., Furneaux, R. H., Grubmeyer, C., Schramm, V. L., and Almo, S. C. (1999) The 2.0 Å structure of human hypoxanthine-guanine phosphoribosyltransferase in complex with a transition-state inhibitor, *Nat. Struct. Biol. 6*, 588−593.
28. Shi, W., Li, C. M., Tyler, P. C., Furneaux, R. H., Cahill, S. M., Girvin, M. E., Grubmeyer, C., Schramm, V. L., Almo, S. C. (1999) The 2.0 Å structure of malarial purine phosphoribosyltransferase in complex with a transition-state analogue inhibitor, *Biochemistry 38*, 9872−9880.
29. Cleland, W. W., and Kreevoy, M. M. (1994) Low-barrier hydrogen bonds and enzymic catalysis, *Science 264*, 1887−1890.
30. Lin, J., Westler, W. M., Cleland, W. W., Markley, J. L., Frey, P. A. (1998) Fractionation factors and activation energies for exchange of the low barrier hydrogen bonding proton in peptidyl trifluoromethyl ketone complexes of chymotrypsin, *Proc. Natl. Acad. Sci. U.S.A. 95*, 14664−14668.
31. Garrett, E. R., and Mehta, P. J. (1972) Solvolysis of adenine nucleosides. I. Effects of sugars and adenine substituents on acid solvolysis, *J. Am. Chem. Soc. 94*, 8532−8541.
32. Mentch, F., Parkin, D. W., and Schramm, V. L. (1987) Transition state structures for N-glycoside hydrolysis of AMP by acid and by AMP nucleosidase in the presence and absence of allosteric activator, *Biochemistry 26*, 921−930.
33. Giblett, E. R., Ammann, A. J., Wara, D. W., Sandman, R., and Diamond, L. K. (1975) Nucleoside-phosphorylase deficiency in a child with severely defective T-cell immunity and normal B-cell immunity, *Lancet 1*, 1010−1013.
34. Kati, W. M., and Wolfenden, R. (1989) Major enhancement of the affinity of an enzyme for a transition state analog by a single hydroxyl group, *Science 243*, 1591−1593.
35. Kati, W. M., Acheson, S. A., and Wolfenden, R. (1992) A transition state in pieces: Contributions of entropic effects to ligand binding by adenosine deaminase, *Biochemistry 31*, 7356−7366.
36. Wolfenden R (1999) Conformational aspects of inhibitor design: enzyme−substrate interactions in the transition state, *Bioorg. Med. Chem. 7*, 647−652.
37. Parkin, D. W., Limberg, G., Tyler, P. C., Furneaux, R. H., Chen, X.-Y., and Schramm, V. L. (1997) Isozyme-specific transition state inhibitors for the trypanosomal nucleoside hydrolases, *Biochemistry 36*, 3528−3534.
38. Basso, L. A., Santos, D. S., Shi, W., Furneaux, R. H., Tyler, P. C., Schramm, V. L., and Blanchard, J. S. (2001) Purine nucleoside phosphorylase from *Mycobacterium tuberculosis*. Analysis of inhibition by a transition state analogue and dissection by parts, *Biochemistry 40*, 8196−8203.
39. Manzumder, D., Kahn, K., and Bruice, T. C. (2002) Computer simulations of trypanosomal nucleoside hydrolase: determination of the protonation state of the bound transition state analogue, *J. Am. Chem. Soc. 124*, 8825−8833.
40. Berti, P. J., and Tanaka, K. S. E. (2002) Transition state analysis using multiple kinetic isotope effects: mechanisms of enzymatic and nonenzymatic glycoside hydrolysis and transfer, *Adv. Phys. Org. Chem. 36*, 239−314.
41. Plateau, P., and Gueron, M. (1982) Exchangeable proton NMR without base-line distortion, using new strong-pulse sequences, *J. Am. Chem. Soc. 104*, 7310−7311.
42. Bax, A., Griffey, R. H., and Hawkins, B. L. (1983) Correlation of proton and nitrogen-15 chemical shifts by multiple quantum NMR, *J. Magn. Reson. 55*, 301−315.

BI026636F